# Probabilistic Definition of Critical Contingencies for Voltage Stability Assessment Considering Correlated Uncertainties

| | |
|---|---|
| Journal: | *Journal of Modern Power Systems and Clean Energy* |
| Manuscript ID | Draft |
| Manuscript Type: | Original Paper |
| Date Submitted by the Author: | n/a |
| Complete List of Authors: | dos Santos, Gustavo; University of Sao Paulo, Electrical and Computer Engineering<br>Nascimento, Matheus; Universidade de São Paulo, Electrical and Computer Engineering<br>Barbosa, João Pedro; Universidade de São Paulo Escola de Engenharia de São Carlos, Electrical and Computer Engineering<br>Oliveira, Maiara; Universidade de São Paulo Escola de Engenharia de São Carlos, Electrical and Computer Engineering<br>pavani, ahda pionkoski Grilo; Universidade Federal do ABC, Centro de Engenharia e Ciências Sociais Aplicadas<br>Ramos, Rodrigo; University of Sao Paulo, Electrical and Computer Engineering |
| Keywords: | voltage stability, probabilistic stability assessment, voltage security margin, critical contingencies, correlated uncertainties, limit-induced bifurcations |
| Speciality: | Stability and Control < Power System Planning, Control and Operation |
| | |

# Probabilistic Definition of Critical Contingencies for Voltage Stability Assessment Considering Correlated Uncertainties

Gustavo G. Santos[1], Matheus R. Nascimento[1], *Member, IEEE*, João Pedro P. Barbosa[1], *Member, IEEE*, Maiara C. Oliveira[1], Ahda P. G. Pavani[2], *Senior Member, IEEE*, and Rodrigo A. Ramos[1], *Senior Member, IEEE*

***Abstract*—The massive integration of intermittent renewable generation and increasing variability of demand raises concerns about the high level of uncertainty in the security assessment of power systems. To address these concerns, this paper proposes a new approach using importance sampling based on the cross-entropy (CE) method to estimate the probability of violations in the voltage security margin of a power system subject to probable contingencies. The CE method is suitable to handle high levels of uncertainty, as it typically provides faster and more accurate results compared to the Monte Carlo simulation, particularly for cases with low probabilities of violations of the voltage security margin. The main contribution of this paper is the proposal of a new definition of critical contingencies, considering uncertainties in the operating conditions that lead to such violations. An important feature of the proposed definition is the consideration of correlated uncertainties with the use of the multivariate normal distribution. Furthermore, the proposed definition is applied to a formulation that is capable of detecting either saddle-node or limit-induced bifurcation with significantly lower simulation times than continuation power flow methods, which is another remarkable feature of this proposal. A proof of concept is presented for a comprehensive explanation of the proposed new definition, followed by an application of this definition to the IEEE 118-bus test system. The findings of this paper highlight the need to carefully select critical contingencies for voltage security assessment in the context of increasing uncertainties.**

***Index Terms*—Voltage stability, probabilistic stability assessment, voltage security margin, critical contingencies, correlated uncertainties, limit-induced bifurcations.**

## I. Introduction

THE decarbonization goals set by several countries around the world are often conflicting with the rapid and diverse growth in power consumption. This issue has been reflected in many types of power system studies, including dynamic stability and security assessment [1]. For example, the Brazilian National System Operator (ONS) reported a record high in the aggregate load of its interconnected system, surpassing 100 GW of peak demand. This high loading of the system was associated with a significant increase in temperature seen in a large part of the country [2]. These extreme climate events are expected to become increasingly frequent and, therefore, it is particularly necessary to quantify and manage the risk of voltage instability due to its relation to high load levels [1].

From a given initial operating condition, voltage stability refers to the ability of a power system to maintain steady voltages at all buses when subjected to a disturbance (e.g., a sustained load buildup) [3]. One of the purposes of voltage stability assessment methods is to determine the distance from the base case to the maximum loadability point. This distance is called voltage stability margin (VSM) [4] and is either calculated with the system structure preserved (i.e., without contingencies) or with probable contingencies [5]. The contingencies can be ranked based on severity by using the VSM results, which are used to select preventive and corrective controls [6], [7].

In analyses using static models, the maximum loadability point is commonly linked to either a saddle-node bifurcation (SNB) or a limit-induced bifurcation (LIB) [8]. An SNB point is identified when the power flow Jacobian matrix has at least one null eigenvalue. A LIB point is mostly observed when a qualitative variation in the system behavior occurs, which can be related, for example, to several synchronous generators reaching their respective reactive power limits ($Q$-limits). After a LIB, the system may become immediately unstable or remain stable. However, the VSM changes abruptly due to the LIB, so $Q$-limits must be considered in VSM calculations, as a LIB may occur before an SNB [8].

System operators around the world rely mostly on variations of the continuation power flow (CPF) [9] to estimate the VSM. However, for contingency analyses, the use of these CPF variants (such as in [10], for example) may involve an excessively high computational burden. The main reasons are the growing uncertainties in the load growth patterns and generation redispatch rules introduced in the problem by the new technologies related to decarbonization. Indeed, the consideration of uncertainties in power system analysis has been a focus of attention of the power systems community recently [5], [11]–[17].

This work was partly supported by the São Paulo Research Foundation (FAPESP) under Grants 2018/20104-9 and 2023/09332-8.

We gratefully acknowledge the support of the RCGI – Research Centre for Greenhouse Gas Innovation (23.1.8493.1.9), hosted by the University of São Paulo (USP), sponsored by FAPESP (2020/15230-5), and sponsored by TotalEnergies, and the strategic importance of the support given by ANP (Brazil's National Oil, Natural Gas and Biofuels Agency) through the R&DI levy regulation. We also acknowledge the support for R&D from TotalEnergies EP Brasil through financing the project "Mitigate curtailment of renewable generation with optimal allocation of energy resources and FACTS in Brazilian Power System" (ANP code 23655-4).

[1]Authors are with the São Carlos School of Engineering of the University of São Paulo, São Carlos, ZIP Code 13566-590, Brazil (e-mail: g.gustavo.santos@usp.br; rmatheus@usp.br; jpeters@usp.br; maiaracoliveira@usp.br; rramos@usp.br).

[2]Ahda P. G. Pavani is with the Center for Engineering and Applied Social Sciences of the Federal University of ABC, Santo André, ZIP Code 09280-560, Brazil (e-mail: ahda.pavani@ufabc.edu.br).

Efficient approaches to calculating the VSM (such as [18], for instance) can be excessively conservative since their goal is to determine the worst-case scenario, with no discussion on the likelihood of its occurrence. A more useful information for system operators is the probability of occurrence of a small VSM, which is directly related to the risk of voltage instability. Considering all possible operating scenarios, those with small VSM are rare instances. Therefore, in a probabilistic framework, importance- sampling techniques are recommended to handle such problems. In particular, the cross-entropy (CE) method has been widely used to enhance the efficiency of Monte Carlo simulation (MCS) in estimating rare events in power systems [19]–[22]. In the context of voltage stability, the works of [21] (which estimates the worst-case scenario) and [22] (which groups critical scenarios) employed the CE method to identify conditions with small VSMs. Both works do not calculate probabilities of occurrence of these VSM, which is a drawback because critical margins with a near-zero probability of occurring may be excessively conservative for operation planning.

This paper proposes a probabilistic approach for voltage security assessment based on a new definition of contingency criticality. A variant of the CE method, considering load and intermittent generation as stochastic variables, is used to calculate the probabilistic VSM in such a way that the output of this proposed CE method forms the basis for the new definition. A normal multivariate probability distribution function (PDF) is employed to consider the correlation of loading and wind farm outputs in nearby areas. A Jacobian matrix expansion strategy is applied to detect both LIB and SNB points. The main contributions are listed below, and they are supported by a proof-of-concept in a 5-bus system and results obtained for the IEEE 118-bus test system.

- In contrast with methods that compute the closest bifurcation point, the proposed approach determines the probabilities of occurrence of VSMs below the security value established by the system operator;
- Based on the calculated probabilities, the proposed definition ranks the criticality of the contingencies in decreasing order in such a way that the resulting list is compliant with grid codes;
- A new direct method based on an expanded Jacobian matrix is introduced for fast and accurate detection of SNB or LIB points, eliminating the need to use the CPF for detecting LIB or an optimization method to solve the stability problem with the $Q$-limit constraints;
- This method uses a multivariate normal probability distribution to consider the correlation matrix associated with generation and load uncertainties. Therefore, it has the advantage of not requiring independent input variables.

The remainder of this paper is structured as follows: Section II provides the mathematical formulation proposed for static voltage stability analysis in this paper; Section III describes the foundations for the models of uncertainties in load and generation in this paper, as well as the variant of the CE method proposed to calculate the probability of violation of the security margin; Section IV presents the proposed approach to define and rank the criticality of contingencies; Section V shows numerical results to comprehensively explain and demonstrate the applicability of the proposed approach; and Section VI outlines the paper conclusions.

## II. Proposed Direct Method to Calculate the Voltage Security Margin

A static nonlinear system model of an electric power system can be formulated as (1). The algebraic power equations in (1) are solved for power flow calculations.

$$\mathbf{f}(\mathbf{z},\lambda)=\mathbf{0},\quad \mathbf{z}\in\mathbb{R}^n,\ \lambda\in\mathbb{R} \tag{1}$$

where $\mathbf{z}$ is the system state vector and $\lambda$ is a parameter associated with active load growth. The bifurcation point at which the system reaches its maximum loadability occurs when $\lambda=\lambda_*$.

In this paper, the maximum loadability point is calculated using a static approach. The VSM calculation problem is solved for a given load growth direction [22] using the proposed direct method, as described in the following.

### A. Mathematical model for load growth direction

For simplicity, the loads are represented by the constant power model, which is commonly employed in static stability analysis since it produces conservative VSM [23]. The apparent power of all loads is assumed to grow as a function of the parameter $\lambda$ with a constant power factor. Thus, the growth of the demanded active power starting from the current operating point can be represented by $\mathbf{P}_L$ and calculated as (2).

$$\mathbf{P}_L=\mathbf{P}_{L0}+\lambda\mathbf{b}_{PL} \tag{2}$$

where $\mathbf{b}_{PL}\in\mathbb{R}^{N_L}$ is the vector of growth directions of $N_L$ and $\mathbf{P}_{L_0}$ is the aggregate of the demanded active power at the current operating point.

This load growth requires the redispatch of non-intermittent generation. The aggregate power output of the non-intermittent generators $\mathbf{P}_G$ is defined by using (3a). Intermittent generation units (such as wind farms) are considered as power injections modeled by stochastic variables, so they are not considered in (3a), which takes only synchronous generators into account.

$$\mathbf{P}_G=\mathbf{P}_{G0}+\boldsymbol{\alpha}\sum_{i=1}^{N_L}\lambda b_{PLi} \tag{3a}$$

$$\alpha_i=\frac{P_{Gi\max}-P_{Gi0}}{\sum_{j=1}^{N_G}(P_{Gk\max}-P_{Gj0})} \tag{3b}$$

where $\boldsymbol{\alpha}=[\alpha_1,\alpha_2,\cdots,\alpha_i,\cdots,\alpha_{N_G}]$ represents the vector of participation factors of $N_G$ synchronous generators according to the rule given by (3b) and $\sum\alpha_i=1$. $P_{Gi0}$, $P_{Gi\max}$, $P_{Gj0}$, and $P_{Gj\max}$ are, respectively, the base case and maximum active power outputs of $i$-th and $j$-th synchronous generators. Since only synchronous generators are redispatched, $\mathbf{P}_{G0}$ is defined in such a way that $\mathbf{P}_{G0}-\mathbf{P}_{L0}$ corresponds to the aggregated power output of non-intermittent generators.

### B. Direct method based on an expanded Jacobian formulation

According to [24], an SNB point, which is characterized by the steady-state Jacobian $\frac{\partial \mathbf{f}}{\partial \mathbf{z}}$ with a single zero eigenvalue can be calculated using the following set of equations.

$$\mathbf{f}(\mathbf{z}_*, \lambda_*) = \mathbf{0} \tag{4a}$$

$$\mathbf{w}^{\mathbf{T}} \left.\frac{\partial \mathbf{f}}{\partial \mathbf{z}}\right|_{(\mathbf{z}_*, \lambda_*)} = \mathbf{0} \tag{4b}$$

$$\|\mathbf{w}\| \neq 0 \tag{4c}$$

where $\mathbf{w}$ is the left eigenvector that must be related to the null eigenvalue at the bifurcation point and $\mathbf{z}_*$ is the state vector when $\lambda = \lambda_*$.

In this paper, the nonzero condition of (4c) is replaced by $\|\mathbf{w}\|^2 - 1 = 0$ to normalize the left eigenvector. The partial derivates of the left eigenvector multiplied by the Jacobian matrix in (4b) are calculated from the expanded Jacobian formulation proposed in [25], which used a variant of the CPF. This formulation uses sigmoid smooth functions to represent the reactive limits of generators and control devices. The result is a direct method capable of finding both SNB and LIB using the same formulation.

For simplicity, in this paper, only control equations involving $Q$-limits were considered, as these are the main causes of LIB. Therefore, the expanded Jacobian matrix is given by

$$\frac{\partial \mathbf{f}}{\partial \mathbf{z}} = \begin{bmatrix} \frac{\partial \mathbf{P}}{\partial \boldsymbol{\theta}} & \frac{\partial \mathbf{P}}{\partial \mathbf{V}} & \mathbf{0} \\ \frac{\partial \mathbf{Q}}{\partial \boldsymbol{\theta}} & \frac{\partial \mathbf{Q}}{\partial \mathbf{V}} & \frac{\partial \mathbf{Q}}{\partial \mathbf{Q}_G} \\ \mathbf{0} & \frac{\partial \mathbf{G}}{\partial \mathbf{V}} & \frac{\partial \mathbf{G}}{\partial \mathbf{Q}_G} \end{bmatrix} \tag{5}$$

where $\mathbf{z} = [\boldsymbol{\theta}, \mathbf{V}, \mathbf{Q}_G]^{\mathbf{T}}$. $\mathbf{P}$, $\mathbf{Q}$, and $\mathbf{G}$ are, respectively, the vectors of active powers, reactive powers, and mismatches of the controlled variables. $\boldsymbol{\theta}$ and $\mathbf{V}$ are vectors with bus voltage angles and magnitudes, respectively, and $\mathbf{Q}_G$ is the control variable vector for the generated reactive powers.

The $Q$-limit control residue of a synchronous generator connected to a bus $k$ can be calculated as (6).

$$\begin{aligned} \Delta G_k = {} & (1 - ch1 \cdot ch3)(1 - ch2 \cdot ch4)(V_k^{\text{ref}} - V_k^{\text{cal}}) \\ & + (ch1 \cdot ch3)(1 - ch2 \cdot ch4)(Q_{Gk}^{\max} - Q_{Gk}) \\ & + (1 - ch1 \cdot ch3)(ch2 \cdot ch4)(Q_{Gk}^{\min} - Q_{Gk}) \end{aligned} \tag{6}$$

where $ch1$, $ch2$, $ch3$, and $ch4$ are sigmoid functions given by

$$ch1 = \left(1 + e^{a(Q_{Gk}^{\text{cal}} - Q_{Gk}^{\max} + tol)}\right)^{-1} \tag{7a}$$

$$ch2 = \left(1 + e^{a(Q_{Gk}^{\text{cal}} - Q_{Gk}^{\min} - tol)}\right)^{-1} \tag{7b}$$

$$ch3 = \left(1 + e^{a(V_k^{\text{cal}} - V_k^{\text{ref}} - tol)}\right)^{-1} \tag{7c}$$

$$ch4 = \left(1 + e^{a(V_k^{\text{cal}} - V_k^{\text{ref}} + tol)}\right)^{-1} \tag{7d}$$

where $Q_G^{\text{cal}}$, $Q_{Gk}^{\max}$, and $Q_{Gk}^{\min}$ are the calculated, maximum, and minimum values of reactive power of bus-$k$ generators. $V_k^{\text{ref}}$ and $V_k^{\text{cal}}$ are the reference and the calculated voltages of bus $k$, respectively, $a$ represents the slope of the sigmoid function, and $tol$ is a tolerance value. To ensure that the outputs of the sigmoid functions are approximately either 0 or 1, $a$ was set to a large value ($> 10^5$) and $tol$ was set to a small one ($< 10^{-4}$).

The objective of the sigmoid functions is to represent the discontinuities related to $Q$-limits by smooth functions, thus enabling the detection of LIB as SNB in (4) [25]. Since the proposed method uses the expanded Jacobian matrix instead of iteratively converting one PV bus into a PQ type according to the PV-PQ bus type switching logic when the reactive power limit is reached, such as in [26], it is simpler to implement and results in significant computation time savings.

The nonlinear algebraic equation set (4), hereinafter described by $\mathbf{F}(\mathbf{Z}) = \mathbf{0}$, with $\mathbf{Z} = [\mathbf{z}, \lambda, \mathbf{w}]$, can be solved by any numerical method. If the classical Newton-Raphson method is used, equation (4b) must be solved for $\mathbf{Z}$, where

$$\frac{\partial \mathbf{F}}{\partial \mathbf{Z}} = \begin{bmatrix} \frac{\partial \mathbf{f}}{\partial \mathbf{z}} & \frac{\partial \mathbf{f}}{\partial \lambda} & \mathbf{0} \\ \frac{\partial (\mathbf{w}^{\mathbf{T}} \cdot \frac{\partial \mathbf{f}}{\partial \mathbf{z}})}{\partial \mathbf{z}} & \mathbf{0} & \frac{\partial (\mathbf{w}^{\mathbf{T}} \cdot \frac{\partial \mathbf{f}}{\partial \mathbf{z}})}{\partial \mathbf{w}} \\ \mathbf{0} & \mathbf{0} & \frac{\partial \left(\|\mathbf{w}\|^2 - 1\right)}{\partial \mathbf{w}} \end{bmatrix} \tag{8}$$

In (8), the terms $\frac{\partial \mathbf{f}}{\partial \lambda}$ and $\frac{\partial \left(\|\mathbf{w}\|^2 - 1\right)}{\partial \mathbf{w}}$ can be replaced by $\mathbf{b}_{PL} - (\boldsymbol{\alpha} \sum_{i=1}^{N_L} b_{PLi})$ and $2 \cdot \mathbf{w}^{\mathbf{T}}$, respectively, and the term $\frac{\partial (\mathbf{w}^{\mathbf{T}} \cdot \frac{\partial \mathbf{f}}{\partial \mathbf{z}})}{\partial \mathbf{w}}$ is equivalent to $\left(\frac{\partial \mathbf{f}}{\partial \mathbf{z}}\right)^{\mathbf{T}}$. Finally, as an extension of [25], the second partial derivative resulting from the application of the Newton-Raphson method to (4b) is calculated as

$$\frac{\partial (\mathbf{w}^{\mathbf{T}} \cdot \frac{\partial \mathbf{f}}{\partial \mathbf{z}})}{\partial \mathbf{z}} = \begin{bmatrix} \frac{\partial \mathbf{A}}{\partial \boldsymbol{\theta}} & \frac{\partial \mathbf{A}}{\partial \mathbf{V}} & \mathbf{0} \\ \frac{\partial \mathbf{B}}{\partial \boldsymbol{\theta}} & \frac{\partial \mathbf{B}}{\partial \mathbf{V}} & \frac{\partial \mathbf{B}}{\partial \mathbf{Q_G}} \\ \mathbf{0} & \frac{\partial \mathbf{C}}{\partial \mathbf{V}} & \frac{\partial \mathbf{C}}{\partial \mathbf{Q_G}} \end{bmatrix} \tag{9}$$

in which

$$\mathbf{A} = \frac{\partial \mathbf{P}}{\partial \boldsymbol{\theta}}^T \cdot \mathbf{w}_P + \frac{\partial \mathbf{Q}}{\partial \boldsymbol{\theta}}^T \cdot \mathbf{w}_Q \tag{10a}$$

$$\mathbf{B} = \frac{\partial \mathbf{P}}{\partial \mathbf{V}}^T \cdot \mathbf{w}_P + \frac{\partial \mathbf{Q}}{\partial \mathbf{V}}^T \cdot \mathbf{w}_Q + \frac{\partial \mathbf{G}}{\partial \mathbf{V}}^T \cdot \mathbf{w}_{Q_G} \tag{10b}$$

$$\mathbf{C} = \frac{\partial \mathbf{Q}}{\partial \mathbf{Q}_G}^T \cdot \mathbf{w}_Q + \frac{\partial \mathbf{G}}{\partial \mathbf{Q}_G}^T \cdot \mathbf{w}_{Q_G} \tag{10c}$$

where $\mathbf{w}_P$, $\mathbf{w}_Q$, and $\mathbf{w}_{QG}$ are the partitions of the left eigenvector $\mathbf{w}$ corresponding to active power, reactive power, and generated reactive power (as a controlled variable).

*Remark:* The expanded Jacobian matrix of (5), with the inclusion of the control variable $\mathbf{Q}_G$, implies that the matrix in (4b) has an extra row and column, as specified by (9). The partial derivatives $\frac{\partial \mathbf{A}}{\partial \boldsymbol{\theta}}$, $\frac{\partial \mathbf{A}}{\partial \mathbf{V}}$ and $\frac{\partial \mathbf{B}}{\partial \boldsymbol{\theta}}$ remain the same. The partial derivatives of the extra row and column are simplified as $\frac{\partial \mathbf{B}}{\partial \mathbf{Q}_G} = \frac{\partial}{\partial \mathbf{V}}\left(\frac{\partial \mathbf{G}}{\partial \mathbf{Q}_G}\right)$; $\frac{\partial \mathbf{C}}{\partial \mathbf{V}} = \frac{\partial}{\partial \mathbf{Q}_G}\left(\frac{\partial \mathbf{G}}{\partial \mathbf{V}}\right)$; and $\frac{\partial \mathbf{C}}{\partial \mathbf{Q}_G} = \frac{\partial^2 \mathbf{G}}{\partial {\mathbf{Q}_G}^2}$. These simplifications contribute to reducing the computational time of the method even further.

## III. Model of Uncertainties in Load and Intermittent Generation

This section defines the uncertain models of load growth and intermittent generation output power, including their stochastic dependence, which is an important feature that must be taken into account in voltage security assessment. For simplicity, only wind generation is considered in this work, but the

proposed approach can be easily modified to accommodate other types of intermittent generation. Then, the use of a CE-based approach is justified and basic concepts related to it are reviewed.

### A. Uncertain model of the load growth direction

Among the multiple load growth models in the literature, a normal PDF (given by (11)) is used in works such as [27] and [28], for example.

$$p(b_{PLi}) = \frac{1}{\sqrt{2\pi\sigma^2_{b_{PLi}}}} \exp\left(-\frac{(b_{PLi}-\mu_{bPLi})^2}{2\sigma^2_{b_{PLi}}}\right) \tag{11}$$

where $\mu_{b_{PLi}}$ and $\sigma_{b_{PLi}}$ are, respectively, the mean and the standard deviation of directions of load increase at bus $i$. To keep a constant power factor, reactive power increases in proportion to active power.

### B. Uncertain model of wind generation

When uncertainties in wind generation are modeled directly in the wind speed, it is common to use a Weibull PDF [28]. However, in [29], the ONS considered historical wind generation data from the northeast region of Brazil and concluded that, when viewed as a group of multiple wind farms, wind generation follows a normal distribution. Indeed, [30] assumes that wind farm (WF) outputs obey a normal PDF and, in [31], the Weibull PDF is approximated by a normal PDF.

This paper follows a line similar to the one adopted in [29]. The wind generation is represented as power injections from wind farm groups and thus modeled by a normal distribution given by (12).

$$p(P_{Wi}) = \frac{1}{\sqrt{2\pi\sigma^2_{P_{Wi}}}} \exp\left(-\frac{(P_{Wi}-\mu_{P_{Wi}})^2}{2\sigma^2_{P_{Wi}}}\right) \tag{12}$$

where $\mu_{P_{Wi}}$ and $\sigma_{P_{Wi}}$ are, respectively, the mean and the standard deviation of wind power generation at bus $i$.

### C. Stochastic dependence among uncertainties

A detailed analysis of the dependence (correlation) of stochastic variables used in VSM assessment can be found in [32]. As a result, the load-to-load correlation is significant, whereas the load-to-wind correlation is negligible. In addition, this reference concludes that the multivariate Gaussian Copula is an accurate representation of the actual data. Since in this paper the uncertainty of wind generation power and load power are both described by normal distributions, using the multivariate normal distribution is equivalent to including the multivariate dependence of the random variables through the Gaussian Copula. Naturally then, for simplicity, a multivariate normal distribution given by (13) was used to account for the interdependence among nearby wind farms and among correlated blocks of load. Wind farms and loads were considered as uncorrelated variables.

$$f(\mathbf{X},\boldsymbol{\mu},\boldsymbol{\Sigma}) = \frac{1}{|\boldsymbol{\Sigma}|(2\pi)^d} \exp\left(-\frac{1}{2}(\mathbf{X}-\boldsymbol{\mu})\boldsymbol{\Sigma}^{-1}(\mathbf{X}-\boldsymbol{\mu})^{\mathbf{T}}\right) \tag{13}$$

where $\mathbf{X} = [\,\mathbf{b_{PL}}\ \mathbf{P_w}\,]$ and $\boldsymbol{\mu} = [\,\boldsymbol{\mu}_{b_{PL}}\ \boldsymbol{\mu}_{P_W}\,]$ are 1-by-d vectors. $\boldsymbol{\Sigma}$ is a d-by-d symmetric, positive definite matrix and $|\boldsymbol{\Sigma}|$ is the determinant of $\boldsymbol{\Sigma}$.

### D. Overview of cross-entropy-based importance sampling

In voltage security assessment, the system is considered insecure if the VSM is smaller than a certain threshold, which will be represented in this paper by $S(\mathbf{X}) \le \gamma$. For instance, the ONS in Brazil defines this threshold as $\gamma$ = 7% for the base case and $\gamma$ = 4% for contingency analyses [33]. Although violations of these security margins can make the system vulnerable to serious outage events with high impact, the probability of occurrence of such violations is typically low [28], [34]. This justifies our decision to assess the risk of voltage insecurity (and instability, consequently) using a CE-based importance sampling technique.

CE-based methods, which involve variance minimization, are known for their effectiveness in estimating probabilities of rare events. Some CE-based power system applications include constrained optimal power flow solutions [19], [20], spinning reserve assessment under transmission constraints [35], and identification of critical scenarios from the voltage stability viewpoint [21], [22].

A brief overview of the proposed CE method is given below. For details on the general fundamentals of the CE method, see [36] and [37]. Let a probability $\ell$ for some measurable function of an event $S(\mathbf{X}) \le \gamma$, $\gamma \in \mathbb{R}$ (i.e., the expectation defined by a collection of indicator functions, $\mathbb{E}\left[I_{\{S(\mathbf{X})\le\gamma\}}\right]$) be defined as

$$\ell = \int I_{\{S(\mathbf{X})\le\gamma\}}\, f(\mathbf{X};\mathbf{u})\, d\mathbf{X}, \quad \mathbf{X} \sim f(\cdot,\mathbf{u}) \tag{14}$$

where $f(\mathbf{X};\mathbf{u})$ is the PDF of $\mathbf{X}$ determined by a parameter vector $\mathbf{u}$, and $I_{\{S(\mathbf{X})\le\gamma\}}$ is the indicator function with a 0 (false) or 1 (true) result.

An estimation of $\ell$ using the Monte Carlo method is given by

$$\hat{\ell} = \frac{1}{N}\sum_{k=1}^{N} I_{\{S(\mathbf{X}_k)\le\gamma\}} \tag{15}$$

which defines an unbiased estimator from $N$ random samples $X_1, X_2, \cdots, X_N$ of a distribution of $\mathbf{X}$.

Consider a new probability distribution $g(\mathbf{X};\mathbf{v})$ so that $\ell$ can be expressed as in (16) and $\hat{\ell}$ estimated by (17).

$$\ell = \int I_{\{S(\mathbf{X})\le\gamma\}} W(\mathbf{X},\mathbf{u},\mathbf{v}) g(\mathbf{X};\mathbf{v}) d\mathbf{X}, \quad \mathbf{X} \sim g(\cdot,\mathbf{v}) \tag{16}$$

$$\hat{\ell} = \frac{1}{N}\sum_{k=1}^{N} I_{\{S(\mathbf{X}_k)\le\gamma\}} W(\mathbf{X}_k,\mathbf{u},\mathbf{v}) \tag{17}$$

where $W(\mathbf{X},\mathbf{u},\mathbf{v}) = f(\mathbf{X},\mathbf{u})/g(\mathbf{X},\mathbf{v})$ is the likelihood ratio of PDFs $f(\mathbf{X};\mathbf{v})$ and $g(\mathbf{X};\mathbf{v})$.

The random samples are now drawn from the distribution $g(\mathbf{X})$ according to (17). Hence, the estimation of PDF $g(\mathbf{X})$ forms the basis of importance sampling techniques. As discussed in Section III-C, in this paper, the used sampling distributions are multivariate normal PDFs. In this case, a fast way to determine $g(\mathbf{X})$ is to select a distribution equivalent

to $f(\mathbf{X})$. To this end, Algorithm 1 describes a CE-based procedure to find $g(\mathbf{X}) \sim f(\mathbf{X};\mathbf{v})$ from the original distribution $f(\mathbf{X};\mathbf{u})$, where $\mathbf{u}$ and $\mathbf{v}$ are the parameter vectors of multivariate normal PDFs (i.e., with mean vector $\boldsymbol{\mu}$ and the correlation matrix $\boldsymbol{\Sigma}$). This algorithm is an adaptation of the original one in [36], with PDF normalization and changes to the convergence criteria. As a result, the computational cost was reduced while also minimizing the potential problems associated with finding a correlation matrix that is not positive definite. It is important to remark that the Cholesky decomposition is required only in the first iteration, so the computational burden of the algorithm is not significantly affected by this decomposition.

**Algorithm 1** Procedure to estimate $\hat{\mathbf{v}}$ of the CE method

1. From $\mathbf{X}$ and its respective PDF $f(\mathbf{X},\mathbf{u})$, generate a set of random samples $\mathbf{X}_j$, $j = 1,\cdots,m$. Convert the random samples $\mathbf{X}_j$ into standard normal values $\mathbf{Z}_j$ and adjust each $\mathbf{Z}_j$ to match the original distribution correlation structure using the Cholesky decomposition. Set $it = 1$ and $\hat{\mathbf{v}}_1 = u$.
2. Calculate the performances $S(\mathbf{X}_j)$ and select the elements $\mathbf{X}_e$, $e = 1,\cdots,m_e$ of the elite set, where $m_e$ is determined by the $p$-th percentile of $m$ sorted in ascending order of their respective $S(\mathbf{X}_e)$.
3. If $S(\mathbf{X}_{m_e}) \leq \gamma$, set $\hat{\mathbf{v}} = \hat{\mathbf{v}}_{it}$ and stop. Otherwise, set $it = it + 1$ and convert the samples $\mathbf{X}_e$ into standard normal values $\mathbf{Z}_e$.
4. Update the parameters $\boldsymbol{\mu}_{it}$ and $\boldsymbol{\Sigma}_{it}$ of $\hat{\mathbf{v}}_{it}$ using $\mathbf{Z}_e$. Then, from PDF $f(\mathbf{Z},\hat{\mathbf{v}}_{it})$ generate new random samples $\mathbf{Z}_j$, $j = 1,\cdots,m$. Convert the standard random samples $\mathbf{Z}_j$ into normal values $\mathbf{X}_j$ using PDF $f(\mathbf{X},\mathbf{u})$. Reiterate from Step 2.

## IV. Proposed Approach to Define Contingency Criticality

As discussed in Section III, this paper proposes a probabilistic approach to analyze the risk of voltage insecurity (and, consequently, voltage instability), with the load and generation uncertainties represented as PDFs. As previously stated, power systems typically operate with large VSM, so violations of this margin are rare events, justifying the use of the CE method. Obviously, when the risk of violation grows, the benefits of CE over the traditional MCS method reduce, but they should still prevail to some extent.

Voltage security and stability studies must be conducted preserving the system structure (without contingencies) and with selected contingencies, considering multiple scenarios of correlated uncertainties. Therefore, to deal with the large number of simulations required, the direct method proposed in Section II was implemented to compute the VSM with an expanded Jacobian matrix, considering the $Q$-limits of the synchronous generators, as described in Section II-B. As previously stated, the main advantage of the proposed implementation is the fact that LIB points are converted to SNB points and become equally identifiable.

The flowchart in Fig. 1 summarizes the steps needed to implement the proposed approach. The input data consists of: (i) network data with line and bus parameters, including the $Q$-limit of synchronous generators; (ii) the number of samples used in each stage of the CE method and the percentage of the elite samples; (iii) parameters of the direct method, such as the maximum mismatch (error) for convergence of the Newton Raphson method; (iv) the mean vector and correlation matrix of the normal multivariate distribution obtained from the load growth direction and the wind generation PDFs; and (v) the lines that will be switched off in contingency analysis. In the flowchart, the variable $c$ represents the contingency number in the list, with $c = 0$ indicating no contingency.

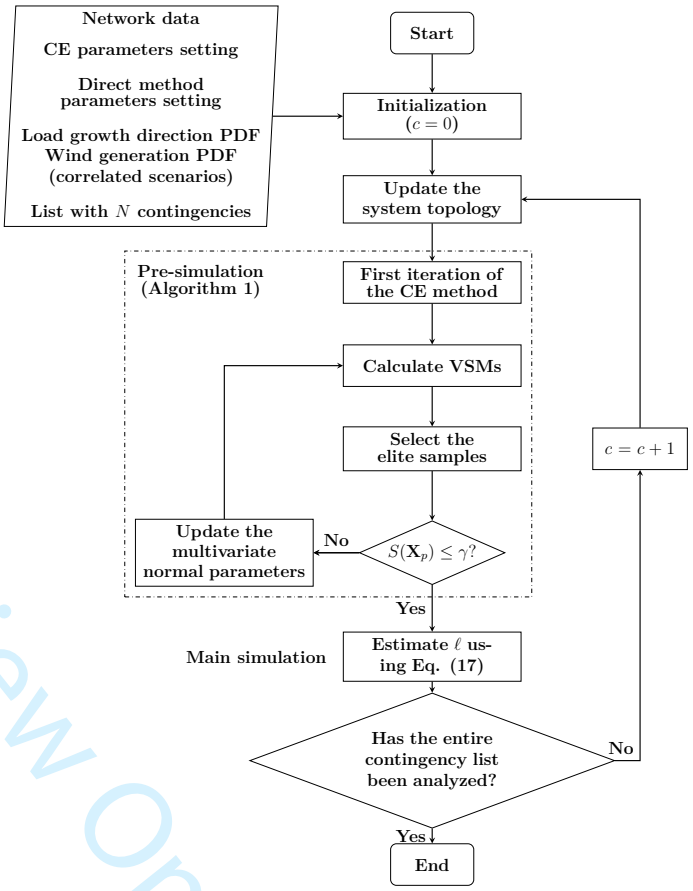


Fig. 1. Flowchart of the proposed CE method.

In the remainder of this paper, Algorithm 1 will be referred to as the pre-simulation stage. The initialization of the proposed CE method generates scenarios (samples) with consumed power from loads and injected power from wind farms using a multivariate normal distribution. For each uncertain scenario and system topology, the proposed direct method is executed to compute the VSMs. As a result, the elite samples are selected from scenarios with the smallest margins. If none of the elite samples violates the voltage security margin, the parameters of the multivariate distribution are updated. In this case, new samples are drawn from updated parameters after a normalization process. Otherwise, the violation probability of the voltage security margin is calculated using the parameters of the current (converged) iteration of the pre-simulation stage. If this stage requires more than one iteration, the likelihood ratio vector must be computed to correct the estimated probability of a violation of the voltage security margin. This procedure is repeated for all topologies and scenarios in the contingency list, where $c = 0$ denotes the system with no contingency.

After the convergence of the pre-simulation stage, the main simulation stage of the proposed CE method produces a list with the probabilities of violation of the voltage security margin for all uncertain operating conditions contained in the contingency list. Based on these probabilities, a new definition of contingency criticality (which is the main contribution of this paper) can be defined as follows.

*Definition:* **When correlated uncertainties in the operating condition are taken into account, the criticality of the selected contingencies must be ranked in decreasing order of their respective probabilities of violation of the voltage security margin.**

As will be shown later in Section V, the main innovation and advantage of this new definition is its compliance with grid codes. Although contingencies happening under operating conditions given by the base case may not result in a violation of the respective voltage security margin, when uncertainties in these conditions are taken into account, the probability of such violation can be quite significant. Therefore, under this framework with correlated uncertainties, a contingency is considered critical if it leads to a probability of violation of the voltage security margin. It is clear that this new definition is compliant with grid codes because it is able to consider that violations of the voltage security margin might occur due to uncertainties even when they are not observed in the base scenario. An illustrative example of this concept is given in subsection V-B.

## V. Simulations and Results

Initially, the proposed method and its advantages are comprehensively explained on a 5-bus test system. As a proof of concept, the bifurcation surface is shown both with and without $Q$-limit consideration, and the results of margin violation probability from the proposed CE method are compared to those obtained using the MCS method to verify the accuracy and the computational efficiency of the former. Although these are known facts in a general sense, this verification is still needed due to the unique characteristics of the voltage stability problem, which involves a nonlinear equation set. Then, the proposed definition of contingency criticality is applied to the IEEE 118-bus test system, which was modified by the addition of seven wind farms. The test results include contingency scenarios, given by topology changes, in addition to the current topology scenario. The violation percentages of $\gamma$ = 7% and $\gamma$ = 4% were used for cases in which the system topology was complete and under contingency, respectively [33]. This application to the IEEE 118-bus system enables an assessment of the advantages of the proposed probabilistic definition of contingency criticality, which is the main contribution of this paper.

### *A. Comprehensive presentation of the application of the proposed CE method on a 5-bus system*

As shown in Fig. 2, this system has generators at buses 1 and 3 and loads at buses 2, 4, and 5. The line parameters and the generator parameters were extracted from [24]. Since the primary goal is the validation of the proposed CE method, a small system with no wind farm was considered. To put the system in a stressed operating condition in the base case, the active and reactive power values consumed by the loads given in [24] were multiplied by 1.7 times their nominal values. Since this test system only has one PV-type bus, we chose a redispatch model in which this bus supplies 23% of the load growth. Furthermore, the reactive power of the generator at bus 3 was limited to 2.5 p.u. As a result, in the scenario with no uncertainties, the load margin was 8.69%.

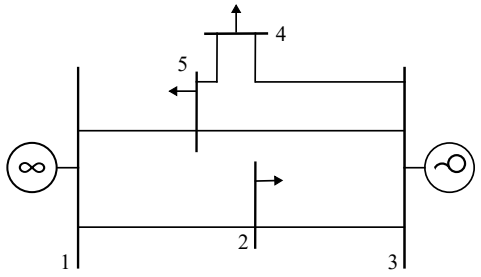


Fig. 2. 5-bus test system

The parameter space of load active powers was mapped in $\mathbb{R}^3$ with $b_{PLi}, i = 2,\ 4$, and 5, ranging from 0 to 1 in intervals of 0.1 p.u. (excluding the direction with no growth), which resulted in 1330 different load growth directions (all starting from the left front corner of Fig. 3). The mapping was carried out disregarding $Q$-limits at first, and then they were considered for comparison purposes. The objective was to illustrate the effect of the $Q$-limits on the bifurcation surface. Fig. 3 clearly shows that $Q$-limits significantly reduce the VSM in all load growth directions.

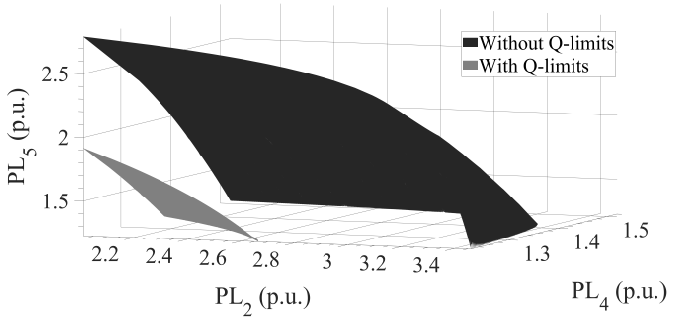


Fig. 3. Bifurcation surfaces of the 5-bus system, with and without $Q$-limits.

When uncertainties in load growth direction are considered, the cases that contain violations of security margins become even rarer events. Hence, more MCS runs imply a better-estimated result, as exhibited in Table I. In this table, the load growth parameter vector $\mathbf{b}_{PL}$ was modeled using a normal distribution with a standard deviation equal to 30% of the nominal load values. For testing and comparison purposes, the correlation matrix among load buses was defined using Pearson correlation coefficients $\rho$ [38] equal to 0 (no correlation), 0.4, and 0.8. The times shown in this table were obtained by simulation on the MATLAB 2022.b software, using a PC with an Intel Core i7-14700 2.1 GHz processor and 32 GB of RAM.

TABLE I
IMPACT OF THE NUMBER OF SAMPLES IN THE SMC RESULTS

| | 3,000 samples | | $10^6$ samples | |
|---|---|---|---|---|
| $\rho$ | P(VSM < 7%) | Time [s] | P(VSM < 7%) | Time [s] |
| **0** | 5.53 | 4.40 | 5.42 | 3,180.87 |
| **0.4** | 2.80 | 4.30 | 2.68 | 2,099.43 |
| **0.8** | 0.60 | 4.23 | 0.48 | 1,813.29 |

In comparison, the results in Table II show the calculated probabilities of violating the 7% VSM when the proposed CE method was used. These results were obtained with $m$ = 750 and $p$ = 0.1 [19] for the pre-simulation stage and 3,000 samples for the main simulation stage. Assuming that the MCS solutions in Table I achieved satisfactory accuracy for the case with $10^6$ samples, it is possible to see that the proposed CE method presented more accurate solutions than the MCS method using 3,000 samples, requiring slightly higher computational times. Furthermore, when compared to the results of the MCS method using $10^6$ samples, the advantages of the proposed CE method in terms of the tradeoff between accuracy and computational time become evident.

TABLE II
RESULTS OF THE PROPOSED CE METHOD

| $\rho$ | P(VSM < 7%) | Time (s) |
|---|---|---|
| **0** | 5.38 | 6.91 |
| **0.4** | 2.55 | 6.69 |
| **0.8** | 0.45 | 6.66 |

The results of Tables I and II for $\rho$ = 0.8 were divided into four intervals to provide more detailed results, as shown in Fig. 4. Each of these intervals is defined by the range to which the voltage security margin of the respective sample belongs, as described by the legend above the figure. Note that the proposed CE method was the closest one to MCS using $10^6$ samples in all intervals. Therefore, Fig. 4 shows that the proposed CE method generates accurate results (when compared to the MCS) for any desired range of violation of the voltage security margin.

### *B. Application of the new definition of contingency criticality to the IEEE 118-bus system*

After the previous section comprehensively explained the proposed CE method, the proposed approach was applied to contingency analysis using the system in Fig. 5 (shown in the next page), in such a way that the proposed definition of contingency criticality can effectively be tested. The active and reactive powers of 99 loads were increased by a factor of 2.15 over the original system values [39] to make it more stressed, and seven wind farms were added to buses 8, 32, 42, 55, 76, 92, and 105. Each wind farm was set to inject 200 MW of active power, so the total amount of power produced by wind farms supplies 15% of the total demand of the system for the base scenario, which leads to a system VSM = 11.54%.

Uncertainties in 99 active power increment values consumed by loads and 7 active power values injected by wind farms

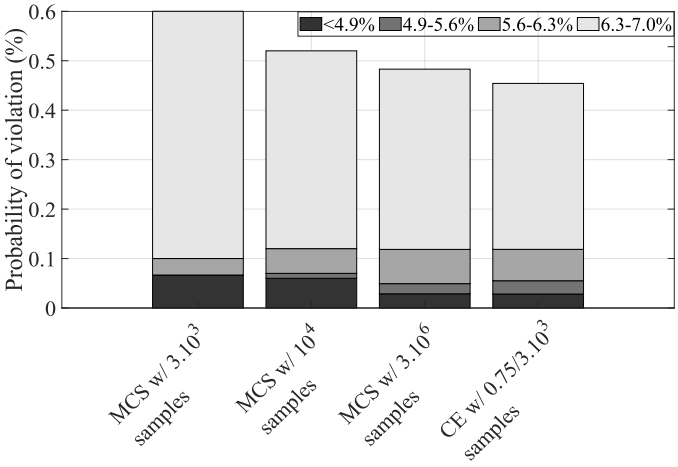


Fig. 4. Results from MCS and CE methods for the case with load correlation given by $\rho = 0.8$.

were considered to calculate the probability of violation of the voltage security margin of the system under contingency. The $\mathbf{b}_{PL}$ parameter was modeled as a normal PDF with a mean value described by the load active powers of the base case and a standard deviation defined as 10% of this mean value. The power injected by each wind farm was modeled as a normal PDF with a mean equal to 200 MW and a standard deviation equal to 25% of this mean. To determine the correlation matrix, this system was first divided into six electrical areas, as shown in Fig. 5. To model load uncertainties, considering that the loads are tightly coupled from both the electrical and geographical perspectives, $\rho$ = 0.8 was used for loads in the same area, $\rho$ = 0.6 for loads in adjacent areas, and $\rho$ = 0.4 otherwise.

The correlation among wind farms, on the other hand, is dependent on their physical proximity. To model this uncertainty, $\rho$ = 0.3 was used for the groups of wind farms connected to buses (8; 32), (42; 55; 76), and (92; 105). The autocorrelation of each wind farm was modeled by $\rho$ = 1 and no correlation ($\rho$ = 0) was considered both between wind farms and loads and between groups of wind farms.

The proposed CE method used 1,000 samples and $p$ = 0.1 for the pre-simulation stage and 10,000 samples for the main simulation stage. In some cases, the pre-simulation stage converged in the first iteration, which indicates that the corresponding events are not rare. In these cases, the parameter $\hat{\boldsymbol{v}}$ is equal to $\mathbf{u}$ and, therefore, the PDF $f(\mathbf{X}, \mathbf{u})$ is suitable for the main simulation stage.

Table III contains the output of the proposed approach, i.e., the list of critical contingencies in descending order according to the new definition proposed to evaluate criticality. For simplicity, only the disconnection of lines was considered in the contingency analysis. In Table III, the third column contains the probability of violation of the voltage security margin that is used to rank the criticality of the contingency considering uncertainties in the operating conditions.

The results in Table III clearly illustrate the importance of considering the proposed definition to adequately rank the contingency list in terms of criticality. If the criterion used to

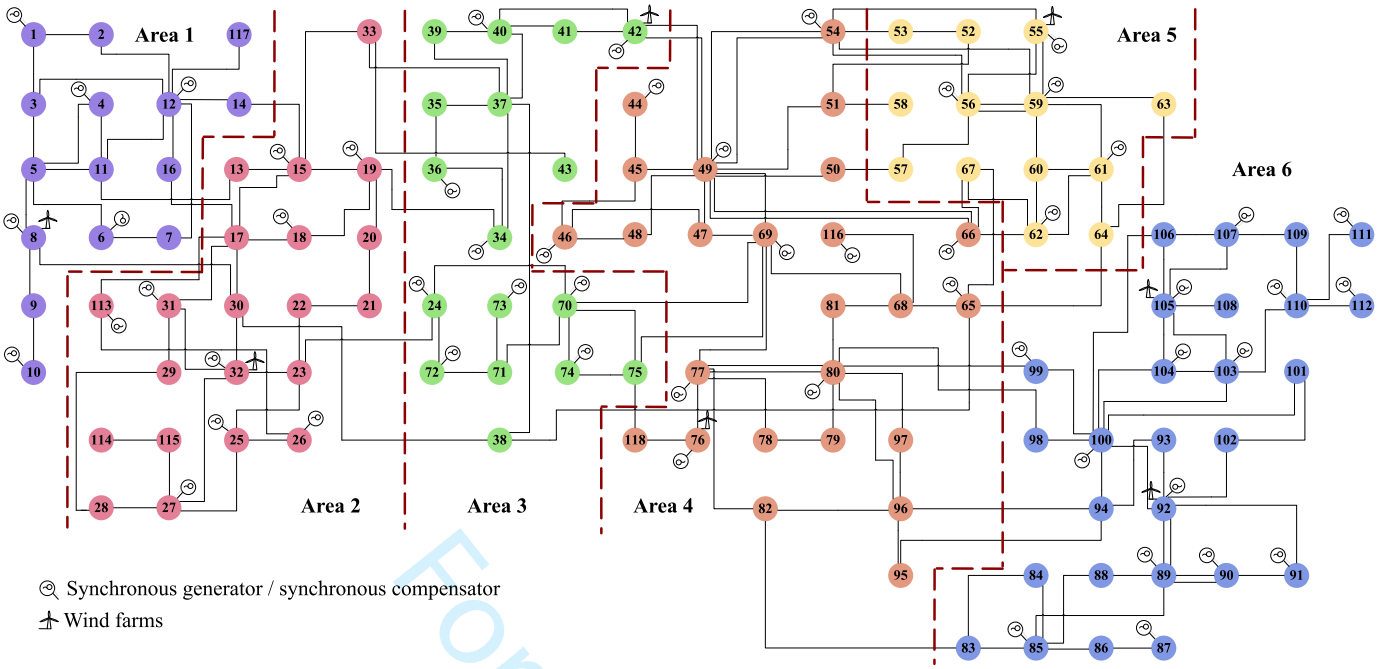


Fig. 5. IEEE 118-bus test system

define criticality is the VSM of the base scenario (which is typically done by system operators), only the contingencies in lines 74-75 and 45-46 would be labeled as critical. Furthermore, the contingencies in lines 22–23 and 44–45 would be prioritized with respect to the ones in lines 75–118, 69–70, and 69–75, for example. These issues could lead to an insufficient determination of preventive control actions to eliminate the critical contingencies in voltage security assessment studies.

TABLE III
OUTPUT OF THE PROPOSED METHOD APPLIED TO THE 118-BUS SYSTEM

| Line under contingency | VSM of the base case | P ($\gamma < 4\%$) with uncertainty |
|---|---|---|
| **Line 74-75*** | 2.07% | 93.84% |
| **Line 45-46*** | 4.05% | 53.95% |
| **Line 75-118*** | 6.12% | 21.73% |
| **Line 69-70*** | 6.49% | 13.84% |
| **Line 69-75*** | 6.72% | 11.25% |
| **Line 44-45** | 5.66% | 4.56% |
| **Line 85-89** | 6.23% | 3.43% |
| **Line 22-23** | 5.32% | 2.45% |
| **Line 85-88** | 7.17% | 1.07% |
| **Line 17-18** | 8.98% | $5.66 \cdot 10^{-5}$% |

* Pre-simulation onverged in the first iteration

In contrast, the definition of criticality proposed in this paper revealed that contingencies with a satisfactory VSM in the base scenario can have a high probability of violation of the voltage security margin due to the uncertainties in the operating conditions. Therefore, it is possible to tailor a threshold for the contingency analysis of interest – depending on the system and its uncertain features, as well as the level of conservatism required by the operator (given that stability and security are at stake) – to consider a probability of violation above which all contingencies must be taken into account for the determination of preventive control actions.

## VI. CONCLUSION

The results of this paper demonstrate the need for adaptation of voltage stability and security assessment methods to the current trends in the operation of power systems, mainly with respect to uncertainties. In particular, the proposed definition of contingency criticality shows that contingencies with satisfactory voltage stability margins in the base case can become critical due to uncertainties in the operating conditions. Thus, with a careful selection of a threshold for the probability of violation of the voltage security margin defined in the respective grid code, it is possible to select and rank the most critical contingencies contained in the list of assessed ones.

However, since uncertainties are considered in the problem formulation, the computational burden to solve it increases. Therefore, to handle this issue, strategies to speed up the solution must be employed. This paper was particularly successful in achieving a satisfactory tradeoff between computational effort and accuracy of the results by proposing a CE-based method to calculate the probability of violations of the VSM. Furthermore, the use of a modified version of the direct method to calculate the VSM also resulted in a reduction of the computational burden.

The proposed definition can be applied to the selection of preventive control actions in order to eliminate the criticality of all contingencies. Furthermore, the definition can be extended to simultaneously assess voltage and small-signal stability and security if Hopf bifurcations are considered in the formulation presented in Section II.

## REFERENCES

[1] J. V. Milanovic, R. Preece, and K. N. Hasan, *Probabilistic Stability Analysis of Uncertain Power Systems*. Wiley-Interscience, 2024.

[2] ONS - Operador Nacional do Sistema Elétrico, "Carga do SIN supera pela primeira vez patamar acima de 100 GW (in portuguese)," Tech. Rep., Nov. 2023. [Online]. Available: https://www.ons.org.br/paginas/noticias/details.aspx?i=9716

[3] N. Hatziargyriou, J. Milanovic, C. Rahmann, V. Ajjarapu, C. Canizares, I. Erlich, D. Hill, I. Hiskens, I. Kamwa, B. Pal, P. Pourbeik, J. Sanchez-Gasca, A. Stankovic, T. Van Cutsem, V. Vittal, and C. Vournas, "Definition and classification of power system stability – revisited & extended," *IEEE Transactions on Power Systems*, vol. 36, no. 4, pp. 3271–3281, Jul. 2021.

[4] Y. Lin, X. Zhang, J. Wang, D. Shi, and D. Bian, "Voltage stability constrained optimal power flow for unbalanced distribution system based on semidefinite programming," *Journal of Modern Power Systems and Clean Energy*, vol. 10, no. 6, pp. 1614–1624, 2022.

[5] D. Guo, L. Wang, T. Jiao, K. Wu, and W. Yang, "Day-ahead voltage-stability-constrained network topology optimization with uncertainties," *Journal of Modern Power Systems and Clean Energy*, vol. 12, no. 3, pp. 730–741, 2024.

[6] M. R. Mansour, L. F. C. Alberto, and R. A. Ramos, "Preventive control design for voltage stability considering multiple critical contingencies," *IEEE Transactions on Power Systems*, vol. 31, no. 2, pp. 1517–1525, Mar. 2016.

[7] M. R. Mansour, E. L. Geraldi, L. F. C. Alberto, and R. A. Ramos, "A new and fast method for preventive control selection in voltage stability analysis," *IEEE Transactions on Power Systems*, vol. 28, no. 4, pp. 4448–4455, Nov. 2013.

[8] L. S. Neves and L. F. C. Alberto, "On the computation of the locally closest bifurcation point considering loading uncertainties and reactive power limits," *IEEE Transactions on Power Systems*, vol. 35, no. 5, pp. 3885–3894, sep 2020.

[9] V. Ajjarapu and C. Christy, "The continuation power flow: a tool for steady state voltage stability analysis," *IEEE Transactions on Power Systems*, vol. 7, no. 1, pp. 416–423, 1992.

[10] R. M. Silva, M. F. Castoldi, A. Goedtel, D. S. Sanches, and R. A. Ramos, "Binary differential evolution applied to the optimization of the voltage stability margin through the selection of corrective control sets," *Soft Computing*, vol. 28, no. 15–16, pp. 8861–8887, Aug. 2023.

[11] A. Akrami, M. Doostizadeh, and F. Aminifar, "Power system flexibility: an overview of emergence to evolution," *Journal of Modern Power Systems and Clean Energy*, vol. 7, no. 5, pp. 987–1007, May 2019.

[12] B. Shakerighadi, F. Aminifar, and S. Afsharnia, "Power systems wide-area voltage stability assessment considering dissimilar load variations and credible contingencies," *Journal of Modern Power Systems and Clean Energy*, vol. 7, no. 1, pp. 78–87, Jun. 2018.

[13] X. Deng, P. Zhang, K. Jin, J. He, X. Wang, and Y. Wang, "Probabilistic load flow method considering large-scale wind power integration," *Journal of Modern Power Systems and Clean Energy*, vol. 7, no. 4, pp. 813–825, Feb. 2019.

[14] Y. Xiang, S. Hu, J. Liu, and R. Wang, "An improved fuzzy method for characterizing wind power," *Journal of Modern Power Systems and Clean Energy*, vol. 9, no. 2, pp. 459–462, 2021.

[15] Y. Zhou, W.-J. Lee, R. Diao, and D. Shi, "Deep reinforcement learning based real-time ac optimal power flow considering uncertainties," *Journal of Modern Power Systems and Clean Energy*, vol. 10, no. 5, pp. 1098–1109, 2022.

[16] Y. Chi, A. Tao, X. Xu, Q. Wang, and N. Zhou, "An adaptive many-objective robust optimization model of dynamic reactive power sources for voltage stability enhancement," *Journal of Modern Power Systems and Clean Energy*, vol. 11, no. 4, pp. 1756–1769, 2023.

[17] W. Wang, M. Wang, X. Han, M. Yang, Q. Wu, and R. Li, "Distributionally robust transmission expansion planning considering uncertainty of contingency probability," *Journal of Modern Power Systems and Clean Energy*, vol. 10, no. 4, pp. 894–901, 2022.

[18] Y. Kataoka, "A probabilistic nodal loading model and worst case solutions for electric power system voltage stability assessment," *IEEE Transactions on Power Systems*, vol. 18, no. 4, pp. 1507–1514, nov 2003.

[19] L. de Magalhaes Carvalho, A. M. Leite da Silva, and V. Miranda, "Security-constrained optimal power flow via cross-entropy method," *IEEE Transactions on Power Systems*, vol. 33, no. 6, pp. 6621–6629, Nov. 2018.

[20] A. M. Leite da Silva and A. M. de Castro, "Risk assessment in probabilistic load flow via monte carlo simulation and cross-entropy method," *IEEE Transactions on Power Systems*, vol. 34, no. 2, pp. 1193–1202, Mar. 2019.

[21] L. M. Alburguetti, R. M. Silva, A. P. Grilo-Pavani, and R. A. Ramos, "Assessment of critical scenarios for voltage stability considering uncertainty of wind power generation," in *2022 IEEE Power & Energy Society General Meeting (PESGM)*. IEEE, jul 2022.

[22] M. R. Nascimento, F. A. Ramos, L. C. Almeida, N. V. C. Gonçalves, A. P. Grilo-Pavani, and R. A. Ramos, "Computation of the minimum voltage stability margin considering loading uncertainties and contingency analysis," in *2023 IEEE Power & Energy Society General Meeting (PESGM)*. IEEE, jul 2023.

[23] E. d. M. Magalhães, A. Bonini Neto, and D. A. Alves, "A parameterization technique for the continuation power flow developed from the analysis of power flow curves," *Mathematical Problems in Engineering*, vol. 2012, no. 1, Jan. 2012.

[24] I. Dobson and L. Lu, "New methods for computing a closest saddle node bifurcation and worst case load power margin for voltage collapse," *IEEE Transactions on Power Systems*, vol. 8, no. 3, pp. 905–913, 1993.

[25] J. P. Peters Barbosa and J. A. Passos Filho, "New methodologies for svc modeling in the power flow problem based on sigmoid functions," *Electrical Engineering*, vol. 106, no. 1, pp. 971–981, Sep. 2023.

[26] T. Jiang, K. Wan, and Z. Feng, "Boundary-derivative direct method for computing saddle node bifurcation points in voltage stability analysis," *International Journal of Electrical Power & Energy Systems*, vol. 112, pp. 199–208, Nov. 2019.

[27] X. Xu, Z. Yan, M. Shahidehpour, H. Wang, and S. Chen, "Power system voltage stability evaluation considering renewable energy with correlated variabilities," *IEEE Transactions on Power Systems*, vol. 33, no. 3, pp. 3236–3245, May 2018.

[28] B. Tan, J. Zhao, and L. Xie, "Transferable deep kernel emulator for probabilistic load margin assessment with topology changes, uncertain renewable generations and loads," *IEEE Transactions on Power Systems*, vol. 38, no. 6, pp. 5740–5754, Nov. 2023.

[29] D. M. Falcão and G. N. Taranto, *Impact of the connections of large-scale wind and solar generation in the brazilian interconnected*, 1st ed. e-papers, 2023.

[30] Y. Yang, S. Lin, Q. Wang, Y. Xie, M. Liu, and Q. Li, "Optimization of static voltage stability margin considering uncertainties of wind power generation," *IEEE Transactions on Power Systems*, vol. 37, no. 6, pp. 4525–4540, Nov. 2022.

[31] A. Baharvandi, J. Aghaei, T. Niknam, M. Shafie-Khah, R. Godina, and J. P. S. Catalao, "Bundled generation and transmission planning under demand and wind generation uncertainty based on a combination of robust and stochastic optimization," *IEEE Transactions on Sustainable Energy*, vol. 9, no. 3, pp. 1477–1486, jul 2018.

[32] M. Alzubaidi, K. N. Hasan, and L. Meegahapola, "Probabilistic steady-state and short-term voltage stability assessment considering correlated system uncertainties," *Electric Power Systems Research*, vol. 228, p. 110008, Mar. 2024.

[33] ONS - Operador Nacional do Sistema Elétrico, *Procedimentos de Rede - Submódulo 2.3 - Premissas, critérios e metodologia para estudos elétricos (in Portuguese)*, Oct. 2022. [Online]. Available: https://www.ons.org.br/paginas/sobre-o-ons/procedimentos-de-rede/vigentes

[34] A. Leite da Silva, I. Coutinho, A. Zambroni de Souza, R. Prada, and A. Rei, "Voltage collapse risk assessment," *Electric Power Systems Research*, vol. 54, no. 3, pp. 221–227, Jun. 2000.

[35] A. M. Leite da Silva, J. F. Costa Castro, and R. A. Gonzalez-Fernandez, "Spinning reserve assessment under transmission constraints based on cross-entropy method," *IEEE Transactions on Power Systems*, vol. 31, no. 2, pp. 1624–1632, Mar. 2016.

[36] R. Y. Rubenstein, *The cross-entropy method*, ser. Information Science and Statistics, D. P. Kroese, Ed. New York, [New York]: Springer, 2004, includes bibliographical references and index. Description based on print version record. "With 38 Illustrations"–Title page.

[37] R. Y. Rubinstein, *Simulation and the Monte Carlo method*, third edition ed., ser. Wiley Series in Probability and Statistics Ser, D. P. Kroese, Ed. Hoboken, New Jersey: Wiley, 2017, no. v.10.

[38] A. G. Asuero, A. Sayago, and A. G. González, "The correlation coefficient: An overview," *Critical Reviews in Analytical Chemistry*, vol. 36, no. 1, pp. 41–59, Jan. 2006.

[39] Power systems test case archive. [Online]. Available: https://labs.ece.uw.edu/pstca/